One-pot Synthesis of (*R*)- and (*S*)-phenylglycinol From Bio-based L-phenylalanine by an Artificial Biocatalytic Cascade

Jiandong Zhang (zhangjiandong@tyut.edu.cn)
Taiyuan University of Technology https://orcid.org/0000-0003-2768-1435

Ning Qi
Department of Biological and Pharmaceutical Engineering, College of Biomedical Engineering, Taiyuan University of Technology, Taiyuan, Shanxi, China

Lili Gao
College of Environmental Science and Engineering, Taiyuan University of Technology, Taiyuan, Shanxi, China

Jing Li
Department of Biological and Pharmaceutical Engineering, College of Biomedical Engineering, Taiyuan University of Technology, Taiyuan, Shanxi, China

Chaofeng Zhang
Department of Biological and Pharmaceutical Engineering, College of Biomedical Engineering, Taiyuan University of Technology, Taiyuan, Shanxi, China

Honghong Chang
Department of Biological and Pharmaceutical Engineering, College of Biomedical Engineering, Taiyuan University of Technology, Taiyuan, Shanxi, China

Research

Keywords: Cascade biocatalysis, L-phenylalanine, Escherichia coli consortia, Chiral phenylglycinol

Posted Date: July 24th, 2021

DOI: https://doi.org/10.21203/rs.3.rs-731971/v1

Abstract

Chiral phenylglycinol is a very important chemical in the pharmaceutical manufacturing. Current methods for synthesis of chiral phenylglycinol often suffered from unsatisfied selectivity, low product yield and using the non-renewable resourced substrates, then the synthesis of chiral phenylglycinol remain a grand challenge. Design and construction of synthetic microbial consortia is a promising strategy to convert bio-based materials to high value-added chiral compounds. In this study, we reported a six-step artificial cascade biocatalysis system for conversion of biobased L-phenylalanine to yield chiral phenylglycinol. The cascade biocatalysis system was conducted by a microbial consortium composed of two engineered recombinant *E*sche*r*ichia *coli* cells modules, one recombinant *E. coli* cell module co-expression of six different enzymes (phenylalanine ammonia lyase/ferulic acid decarboxylase/phenylacrylic acid decarboxylase/styrene monooxygenase/epoxide hydrolase/alcohol dehydrogenase) for efficient conversion of L-phenylalanine into 2-hydroxyacetophenone. The second recombinant *E. coli* cell module expression of an (*R*)-ω-transaminase or co-expression of the (*S*)-ω-transaminase, alanine dehydrogenase and glucose dehydrogenase for conversion of 2-hydroxyacetophenone to (*S*)- or (*R*)-phenylglycinol, respectively. Combining the two engineered *E. coli* cell modules, after the optimization of bioconversion conditions (including pH, temperature, glucose concentration, amine donor concentration and cell ratio), L-phenylalanine could be easily converted to (*R*)-phenylglycinol and (*S*)-phenylglycinol with up to 99% conversion and >99% *ee*. Preparative scale biotransformation was also conducted on 100 mL scale, (*S*)-phenylglycinol and (*R*)-phenylglycinol were obtained in 71.0% and 80.5% yield, >99% *ee*, and 5.19 g/L.d and 4.42 g/L.d productivity, respectively. The salient features of this biocatalytic cascade system are good yields, excellent *ee*, mild reaction conditions and no need for additional cofactor ($NADH/NAD^+$), provide a practical biocatalytic method for sustainable synthesis of (*S*)-phenylglycinol and (*R*)-phenylglycinol from biobased L-phenylalanine.

Introduction

Chiral vicinal amino alcohol moieties are important structural features of many pharmaceutically active molecules and natural products (Bergmeier et al. 2000; Gupta et al. 2018), besides, they can be used as chiral ligands or auxiliaries in asymmetric synthesis (Tan et al. 2017). In this context, enantiopure phenylglycinols are particularly interesting due to their potential use as a key building block for many pharmaceuticals synthesis, such as neurotrophic agent (Panek et al. 1998), h5-HT1D receptor agonists (Russell et al. 1999), antimitotic agents (Kim, et al. 2004) and p21-activated kinases (PAK4) inhibitors (Guo et al. 2017).

The industrial synthesis of vicinal amino alcohol typically uses chemical methods. Such as reduction of amino acids (McKennon et al. 1993; Vandekerkhove et al. 2018), asymmetric ring opening of epoxides (Overman et al. 1985; Jacobsen et al. 2000), addition of lithiated aziridines to boronic esters (Schmidt et al. 2009), addition of nucleophiles to aminocarbonyls (Reetz et al. 1991) and imines (Kobayashi et al. 1998) and Sharpless's osmium-catalysed asymmetric aminohydroxylation (AA) of styrene (Li et al. 1996; Sharpless et al. 1975). However, chemical methods for synthesis of chiral vicinal amino alcohol often

suffered from unsatisfied regioselectivity and enantioselectivity, low product yield, the expense and toxicity of metal catalyst and N-protected amino alcohol product, made these methods unsatisfactory for industrial application. In comparison, biocatalysis as a more sustainable method has been widely used in the synthesis of many useful chemicals (You et al. 2021; Wang et al. 2020). In the past two decades, various biocatalytic ways have been reported for the synthesis of chiral vicinal amino alcohols, such as racemic amino alcohol kinetic resolution (Wu et al. 2017; Rouf et al. 2011), chiral amino ketones asymmetric reduction (Patel et al. 1993) and α-ketol asymmetric reduction amination (Zhang et al. 2019a; Chen et al. 2019). Recently, two types of biocatalytic cascades for asymmetric ring-opening of epoxides (Zhang et al. 2019b) and asymmetric aminohydroxylation of alkene (Zhang et al. 2020) have been developed for the synthesis of chiral vicinal amino alcohols, good conversions (up to 99%) and excellent *ee* (> 99%) of products were obtained from the tested epoxides and alkenes. Despite the substrates (epoxide and alkene) used in these methods are not expensive and readily available, the epoxides and alkenes are mainly produced from the fossil (non-renewable carbon resources) resource, make these methods less sustainable. As such, there is a drive to find new biocatalytic strategies for synthesizing chiral vicinal amino alcohols from sustainably resourced substrates.

L-α-amino acids are bio-based materials can be produced from the fermentation of carbohydrates or waste protein sources (Pelckmans et al. 2017). According to statistics, the annual worldwide amino acids production is estimated at over four million tons (Becker et al. 2012). Therefore, the bio-based L-α-amino acids will make a significant contribution to the economic and ecological production of chemical products and materials. In the past decades, a lot of methods have been developed for conversion of L-α-amino acids into other high value-added compounds (Fotheringham et al. 2006; Studte et al. 2008; Zhang et al. 2019c). For example, cascade biocatalysis for conversion of L-phenylalanine to chiral styrene oxide, 1-phenylethane-1,2-diol, mandelic acid, phenylglycine have been reported (Zhou et al. 2016). An *in vivo* four-enzyme cascade pathway was constructed for the synthesis of D-*p*-hydrophenylglycine from L-tyrosine, 92.5% conversion and > 99% ee of D-*p*-hydrophenylglycine was obtained from 50 g/L L-tyrosine (Tan et al. 2021). A whole-cell cascade biocatalysis system was established for efficient production of glutarate from L-lysine with the recombinant *E. coli* microbial consortium, 43.8 g/L glutarate could be obtained via a fed-batch strategy (Wang et al. 2019). Very recently, a first one pot cascade biotransformation of L-phenylalanine to chiral phenylglycinol have been developed, 42% conversion of (*R*)-phenylglycinol (99% *ee*) and 26% conversion of (*S*)-phenylglycinol (92% *ee*) were obtained from L-phenylalanine by engineered *E. coli* strains (Sekar et al. 2020). Unfortunately, the low substrate loading, the low productivity and unsatisfactory *ee* of product significantly limit industrial application of this process. The development of a highly efficient biocatalysis system for the synthesis of chiral phenylglycinol from L-phenylalanine remains challenging.

In this study, a novel artificial designed cascade biocatalysis system was constructed for conversion of biobased L-phenylalanine to yield chiral phenylglycinol. The cascade biocatalysis was conducted by using a microbial consortium including two recombinant *E. coli* cell modules (Scheme 1). One *E. coli* cell module co-expression of the phenylalanine ammonia lyase (PAL), phenylacrylic acid decarboxylase (PAD), styrene monooxygenase (SMO), epoxide hydrolase (EH) and alcohol dehydrogenase (ADH) for

conversion of L-phenylalanine (L-PA, **1**) to 2-hydroxyacetophenone (2-HAP, **6**). The second recombinant *E. coli* cell module (module 2 or module 3) expressing an ω-transaminase for conversion of 2-HAP to chiral phenylglycinol. The recombinant *E. coli* cell module **2** expressing an (*R*)-selective ω-transaminase was used for conversion of 2-HAP to (*S*)-phenylglycinol. The recombinant *E. coli* cell module **3** co-expression of (*S*)-selective ω-transaminase, alanine dehydrogenase (AlaDH) and glucose dehydrogenase (GDH) was employed for conversion 2-HAP to (*R*)-phenylglycinol. Combining the two recombinant *E. coli* modules (module 1/module 2 or module 1/module 3), L-phenylalanine could be easily converted to (*R*)-phenylglycinol and (*S*)-phenylglycinol with good conversion and excellent *ee*.

Materials And Methods

Chemicals

L-phenylalanine (L-PA), *trans*-cinnamic acid, styrene, (*S*)-1-phenyl-1, 2-ethanediol, styrene oxide, 2-hydroxyacetophenone (2-HAP), (±)-phenylglycinol, (*R*)-phenylglycinol, (*S*)-phenylglycinol, L-alanine (L-Ala), *n*-dodecane, pyridoxal-5'-phosphate (PLP) and (*R*)-α-methylbenzylamine (R-MBA) were from Energy Chemical and Titan Scientific (Shanghai, China). Yeast extract, Tryptone and antibiotics (kanamycin, ampicillin and streptomycin) were from Sangon Biotech (Shanghai, China). T4 DNA ligase and restriction enzymes were from New England Biolabs (NEB, Beijing, China). Isopropyl β-D-1-thiogalactopyranoside (IPTG) and Taq plus DNA polymerase were purchased from Tsingke (Beijing, China). All other chemical reagents were obtained from commercial sources.

Plasmids, microorganisms and media

The expression plasmids (pET28a (+), pETduet-1, pRSFduet-1 and pCDFduet-1) were from Novagen (Madison, WI, USA). Previously constructed recombinant plasmids (pET28a-SMO, pETduet-SpEH, pET28a-GoSCR, pET28a-MVTA, pET28a-BMTA and pETduet-GDH) (Zhang et al. 2020) were stored in our lab. The host strain *E. coli* T7 supercompetent cells were purchased from NEB (Beijing, China). The *E. coli* strains were grown at 37°C in Luria-Bertani (LB) medium or Terrific Broth (TB) medium. Antibiotics ampicillin (0.1 mg/mL), kanamycin (0.05 mg/mL) and streptomycin (0.1 mg/mL) were utilized for the selection of recombinant *E. coli* cells. *Bacillus subtilis* sp. 168 stored in our lab was maintained on MRS agar slants and grown in MRS medium at 30°C.

Construction of the recombinant E. coli strains

All the primers used in this study were synthesized by Tsingke (Beijing, China) and list in Additional file 1: Table S1. All the constructed plasmids and recombinant *E. coli* cells were list in Additional file 1: Table S2. *E. coli* (GoSCR), *E. coli* (GDH) (Cui et al. 2017), *E. coli* (MVTA) (Zhang et al. 2019a), *E. coli* (SpEH) (Zhang et al. 2019b), *E. coli* (SMO) and *E. coli* (BMTA) (Zhang et al. 2020) were constructed as described previously.

For *E. coli* (PAL), *E. coli* (Fdc1) and *E. coli* (Pad1), the phenylalanine ammonia lyase (PAL) gene from *Arabidopsis thaliana* (Cochrane et al. 2004), the ferulic acid decarboxylase (Fdc1) gene and phenylacrylic acid decarboxylase (Pad1) gene from *Aspergillus niger* (Payne et al. 2015) were synthesized and inserted into the expression vector pET28a at the *Nde*I/*Xho*I sites by Tsingke (Beijing, China), respectively. The resulting recombinant plasmids, pET28a-PAL, pET28a-Fdc1 and pET28a-Pad1 were separately transformed into competent *E. coli* T7 to form *E. coli* (PAL), *E. coli* (Fdc1) and *E. coli* (Pad1).

For *E. coli* (AlaDH), the genome DNA was extracted from *Bacillus subtilis* sp. 168 by using Bacterial DNA extraction kit (Sangon Biotech, China). The DNA fragment of AlaDH gene was amplified from the genomic DNA of *Bacillus subtilis* sp. 168 by standard polymerase chain reaction (PCR) using the primers listed in Additional file 1: Table S1. The PCR product was inserted into the expression vector pETduet-1 at the *BamH*I/*Pst*I sites to form pETduet-AlaDH. Then the constructed recombinant plasmid pETduet-AlaDH was transformed into competent *E. coli* T7 to form recombinant *E. coli* (pETduet-AlaDH). In a similar way, the recombinant *E. coli* (pCDFduet-AlaDH) was constructed.

For *E. coli* (Fdc1-Pad1), the DNA fragment of Fdc1 and Pad1 were amplified by PCR using the primers listed in Additional file 1: Table S1. Fdc1 gene was double-digested with the *BamH*I and *Not*I and inserted into pRSFduet-1 to form pRSFduet-Fdc1. Then the Pad1 gene was double-digested with the *Nde*I and *Xho*I, and inserted into pRSFduet-Fdc1 to form pRSFduet-Fdc1-Pad1 (For convenience, RFP was used instead). The recombinant plasmid pRSFduet-Fdc1-Pad1 was then transformed into competent *E. coli* T7 to form the recombinant *E. coli* (pRSFduet-Fdc1-Pad1) cells (designated as *E. coli* (RFP)). Similarly, the recombinant *E. coli* (pETduet-Fdc1-Pad1) (designated as *E. coli* (DFP)) and *E. coli* (pCDFduet-Fdc1-Pad1) (designated as *E. coli* (CFP)) were constructed in the same way.

For *E. coli* (pETduet-SpEH-PAL), the DNA fragment of SpEH and PAL were amplified by PCR using the primers listed in Additional file 1: Table S1. SpEH gene was double-digested with the *BamH*I and *Hind*III and inserted into pETduet-1 to form pETduet-SpEH. Then PAL gene was double-digested with the *Nde*I and *Xho*I and inserted into pETduet-SpEH to form pETduet-SpEH-PAL (For convenience, DEA was used instead). The recombinant plasmid pETduet-SpEH-PAL was transformed into competent *E. coli* T7 to form *E. coli* (pETduet-SpEH-PAL) (designated as *E. coli* (DEA)).

Similarly, the recombinant *E. coli* (pCDFduet-PAL-SMO) (designated as *E. coli* (CAS)), *E. coli* (pRSFduet-SpEH-GoSCR) (designated as *E. coli* (REG)), *E. coli* (pCDFduet-GoSCR-SMO) (designated as *E. coli* (CGS)), *E. coli* (pETduet-SpEH-SMO) (designated as *E. coli* (DES)), *E. coli* (pRSFduet-GoSCR-PAL) (designated as *E. coli* (RGA)) were constructed in the same way.

For *E. coli* (PAL-Fdc1-Pad1-SMO-SpEH-GoSCR), the constructed recombinant plasmids pRSFduet-Fdc1-Pad1, pETduet-SpEH-PAL and pCDFduet-GoSCR-SMO with different antibiotic resistance were simultaneously transformed into the competent *E. coli* T7 to form the recombinant *E. coli* (PAL-Fdc1-Pad1-SMO-SpEH-GoSCR) cells (designated as *E. coli* (RFP-DEA-CGS). Similarly, the recombinant *E. coli* (DFP-CAS-REG) and *E. coli* (CFP-DES-RGA) cells co-expressing of PAL, Fdc1, Pad1, SMO, SpEH and GoSCR were constructed in the same way with the different recombinant plasmid combinations.

For *E. coli* (pETduet-GDH-AlaDH), the GDH and AlaDH genes were amplified by PCR using the primers listed in Additional file 1: Table S1. GDH gene was double-digested with *BamH*I and *Hind*III and inserted into pETduet-1 to form pETduet-GDH. Then AlaDH gene was double-digested with restriction endonucleases of *Kpn*I and *Xho*I and inserted into pETduet-GDH to obtain a new recombinant plasmid pETduet-GDH-AlaDH (For convenience, DGA was used instead). The recombinant plasmid pETduet-GDH-AlaDH was then transformed into the competent *E. coli* T7 to form recombinant *E. coli* (pETduet-GDH-AlaDH) (designated as *E. coli* (DGA)).

For *E. coli* (BMTA-GDH-AlaDH), the constructed recombinant plasmids pET28a-BMTA and pETduet-GDH-AlaDH with different antibiotic resistance were simultaneously transformed into the competent *E. coli* T7 to form recombinant *E. coli* (BMTA-GDH-AlaDH) (designated as *E. coli* (EB-DGA)). Similarly, the recombinant plasmids pET28a-BMTA, pETduet-GDH and pCDFduet-AlaDH were simultaneously transformed into the competent *E. coli* T7 to form recombinant *E. coli* (BMTA-GDH-AlaDH) (designated as *E. coli* (EB-DG-CA)).

The expression of all genes from above constructed recombinant *E. coli* strains was confirmed by sodium dodecyl sulfate polyacrylamide gel electrophoresis (SDS-PAGE) and testing the activity of corresponding enzymes.

Enzyme expression and activity analysis

The constructed recombinant *E. coli* cells were cultivated at 37°C for 12 h in 5 mL LB medium (10 g/L peptone, 5 g/L yeast extract and 10 g/L NaCl, pH7.0) containing appropriate antibiotics. Two milliliter of seed culture was then inoculated into 100 mL of Terrific Broth (TB) medium (12 g/L tryptone, 24 g/L yeast extract, 4 g/L glycerol, 17 mM KH_2PO_4, 72 mM K_2HPO_4) supplemented with the appropriate antibiotics, and cultivated at 37°C for 2–3 h. When OD_{600} value of the recombinant *E. coli* cells reached 0.6 – 0.8, IPTG (0.5 mM) was then added to the medium to induce the protein expression. After incubation for 12 – 20 h at 20°C and 200 rpm, cells were harvested by centrifugation (8,000 rpm) at 4°C for 10 min, washed twice with cold saline and resuspended in sodium phosphate buffer (100 mM, pH 7.5). The cell pellets were disrupted with ultra-sonication for 20 min. The cell debris were removed by centrifugation (12,000 rpm, 30 min) at 4°C, and the soluble portion of cell lysate was stored at − 80°C for further use.

The activity of phenylalanine ammonia lyase (PAL) was measured as described previously (Cochrane et al. 2004). The reaction mixture consisted of 100 mM sodium phosphate buffer (pH 8.5), 5 mM L-phenylalanine substrates, and an appropriate amount of enzyme in a total volume of 0.5 mL. The reaction was incubated at 30°C for 5 min. 100 μL reaction mixture extracted with acetonitrile (900 μL) containing 2 mM acetophenone (internal standard). The concentration of the *trans*-cinnamic acid was determined by HPLC analysis. 1 unit of activity refers to the amount of catalyst that catalyzed the conversion of 1 μmol L-phenylalanine to *trans*-cinnamic acid per min.

The activity of decarboxylases (Fdc1 and Pad1) was measured as described previously (Payne et al. 2015). The reaction mixture consisted of 100 mM sodium phosphate buffer (pH 7.0), 5 mM *trans*-

cinnamic acid, and an appropriate amount of enzyme in a total volume of 0.5 mL. After the reaction mixture was incubated at 30°C for 5 min. Sample (100 μL) was extracted with acetonitrile (900 μL) containing 2 mM acetophenone (internal standard). The concentration of the styrene was determined by HPLC analysis. 1 unit of activity refers to the amount of catalyst that catalyzed the conversion of 1 μmol *trans*-cinnamic acid to styrene per min.

The activity of styrene monooxygenase (SMO) was measured as described previously (Xu et al. 2009). The reaction mixture consisted of 100 mM sodium phosphate buffer (pH 7.0), 5 mM styrene substrate, 1 mM NADH, and an appropriate amount of enzyme in a total volume of 0.5 mL. After incubation at 30°C for 5 min. The concentration of styrene oxide was determined by GC analysis. 1 unit of activity refers to the amount of catalyst that catalyzed the conversion of 1 μmol styrene to styrene oxide per min.

The activity of epoxide hydrolase (SpEH) was measured as described previously (Wu et al. 2013). The reaction mixture consisted of 100 mM sodium phosphate buffer (pH 7.0), 10 mM styrene oxide substrate, and an appropriate amount of enzyme in a total volume of 0.5 mL. After incubation at 30°C for 5 min. The concentration of the 1-phenyl-1,2-ethanediol was determined by GC analysis. 1 unit of activity refers to the amount of catalyst that catalyzed the conversion of 1 μmol styrene oxide to 1-phenyl-1,2-ethanediol per min.

The oxidation activity of alcohol dehydrogenase was measured as described previously (Zhang et al. 2020). The reaction mixture consisted of 100 mM sodium phosphate buffer (pH 7.5), 0.2 mM NAD^+, 10 mM 1-phenyl-1,2-ethanediol and an appropriate amount of enzyme in a total volume of 1.0 mL, the reaction was performed at 30°C for 1 min. 1 unit of activity refers to the amount of catalyst that catalyzed the conversion of 1 μmol NAD^+ to NADH per min.

The activity of alanine dehydrogenase (AlaDH) was measured as described previously (Lerchner et al. 2016). The reaction mixture consisted of 100 mM sodium phosphate buffer (pH 7.5), 0.2 mM NADH, 5 mM pyruvate, 200 mM NH_4Ac and an appropriate amount of enzyme in a total volume of 1.0 mL. The reaction was performed at 30°C for 1 min. 1 unit of activity refers to the amount of catalyst that catalyzed the conversion of 1 μmol NADH to NAD^+ per min.

The activity of transaminase was assayed as described in our previous study (Zhang et al. 2017). The activity of glucose dehydrogenase (GDH) was measured as described in our previous study (Cui et al. 2017).

The activity of recombinant *E. coli* (DFP-CAS-REG) cells was measured by testing the formation of 2-HAP **6**. The reaction mixture consisted of 100 mM sodium phosphate buffer (pH 7.5), 10 mM L-PA **1**, 10 mM glucose and 5 g cell dry weight (cdw)/L recombinant *E. coli* cells in a total volume of 1.0 mL, the reaction was performed at 25°C and 200 rpm for 10 min. The concentration of 2-HAP was determined by GC analysis. 1 unit of activity refers to the amount of catalyst that catalyzed the conversion of 1 μmol L-PA to 2-HAP per min.

The protein concentration was determined by the Bradford method (Bradford, 1975).

In vitro **conversion of L-PA 1 to 2-HAP 6 and chiral phenylglycinol 7**

The freshly prepared recombinant *E. coli* cells (*E. coli* (PAL), *E. coli* (Fdc1), *E. coli* (Pad1), *E. coli* (SMO), *E. coli* (SpEH), *E. coli* (GoSCR), *E. coli* (BMTA) and *E. coli* (MVTA)) were washed two times with sterile deionized water, and resuspended in sterile deionized water to an OD_{600} of 50, respectively. The cell pellets were disrupted with ultra-sonication for 20 min. After centrifugation for 30 min at 4°C and 12,000 rpm, the cell debris was removed. The soluble portion of cell lysate was frozen at − 80°C overnight. Then the frozen cell free extracts were lyophilized by vacuum freeze dryer. For conversion of L-PA **1** to 2-HAP **6**, the reaction mixture consisted of 100 mM of sodium phosphate buffer (pH 7.5), 10–20 mM of L-PA, 0.5 mM of NADH, 15 mg/mL of PAL, 15 mg/mL of Fdc1, 15 mg/mL of Pad1, 20 mg/mL of SMO, 10 mg/mL of SpEH, 20 mg/mL of GoSCR in a total volume of 5 mL. For conversion of L-PA **1** to phenylglycinol **7**, the reaction mixture consisted of 100 mM of sodium phosphate buffer (pH 7.5), 10–20 mM of L-PA **1**, 0.5 mM of NADH, 15 mg/mL of PAL, 15 mg/mL of Fdc1, 15 mg/mL of Pad1, 20 mg/mL of SMO, 10 mg/mL of SpEH, 20 mg/mL of GoSCR, 15 mg/mL of MVTA or 15 mg/mL of BMTA, 0.1 mM of PLP, and 15–25 mM of (*R*)-MBA or 200 mM of L-Ala in a total volume of 5 mL. The reactions were conducted at 30°C and 200 rpm. At appropriate intervals, samples were taken for GC analysis.

In vivo **conversion of L-PA 1 to 2-HAP 6 with the resting cells of recombinant** E. coli **cells**

The freshly prepared recombinant *E. coli* (RFP-DEA-CGS), *E. coli* (DFP-CAS-REG) and *E. coli* (CFP-DES-RGA) cells were frozen at − 80°C overnight and lyophilized to get the cell powders. The reaction mixture consisted of 100 mM sodium phosphate buffer (pH 7.5), 10 g cdw/L of lyophilized recombinant *E. coli* cells, 10 mM of L-PA **1** and 10 mM of glucose in a total volume of 5 mL. The reactions were performed at 25°C and 200 rpm. At appropriate intervals, samples were taken for GC analysis.

In vivo **conversion of 2-HAP 6 to (**S**)- or (**R**)-phenylglycinol 7**

The freshly prepared recombinant *E. coli* (MVTA) and *E. coli* (EB-DGA) cells were frozen at − 80°C overnight and lyophilized to get the cell powders. The reaction mixture consisted of 100 mM sodium phosphate buffer (pH 8.0), 10 g cdw/L of lyophilized recombinant *E. coli* cells, 10 mM of 2-HAP **6**, 0.1 mM PLP, 10% DMSO, 20 mM R-MBA or 400 mM L-Ala (including 150 mM NH_3/NH_4Cl) in a total volume of 5 mL. The reactions were performed at 30°C and 200 rpm. At appropriate intervals, samples were taken for GC analysis.

Conversion of L-PA 1 to (S **)-phenylglycinol 7 with the mixture of resting cells of** E. coli **(RFP-DEA-CGS) and** E. coli **(MVTA)**

The reaction mixture consisted of 100 mM sodium phosphate buffer (pH 8.0), 20 g cdw/L of lyophilized recombinant *E. coli* (RFP-DEA-CGS) cells, 15 g cdw/L of lyophilized recombinant *E. coli* (MVTA) cells, 10–50 mM of L-PA **1**, 5–40 mM of glucose, 0.1 mM of PLP, 25–40 mM of (*R*)-MBA in a total volume of 5 mL.

The reactions were performed at 25°C and 200 rpm. At appropriate intervals, samples were taken for GC analysis.

Conversion of L-PA 1 to (R **)-phenylglycinol 7 with the mixture of resting cells of** E. coli **(RFP-DEA-CGS) and** E. coli **(EB-DGA)**

The reaction mixture consisted of 100 mM sodium phosphate buffer (pH 8.0), 15 g cdw/L of lyophilized recombinant *E. coli* (RFP-DEA-CGS) cells, 20 g cdw/L of lyophilized recombinant *E. coli* (EB-DGA) cells, 10–50 of mM L-PA **1**, 5–40 mM of glucose, 0.1 mM of PLP, 100–600 mM of L-Ala and 0-200 mM of NH_3/NH_4Cl in a total volume of 5 mL. The reactions were performed at 25°C and 200 rpm. At appropriate intervals, samples were taken for GC analysis.

Preparation experiment

For preparation of (*S*)-phenylglycinol **7**, the reaction was conducted in 100 mL sodium phosphate buffer (100 mM, pH 7.5) containing 20 mM (330.4 mg) of L-PA **1**, 20 g cdw/L of *E. coli* (RFP-DEA-CGS), 15 g cdw/L of *E. coli* (MVTA), 10 mM of glucose, 0.1 mM of PLP and 30 mM of (*R*)-MBA. For preparation of (*R*)-phenylglycinol **7**, the reaction was conducted in 100 mL sodium phosphate buffer (100 mM, pH 7.5) containing 20 mM (330.4 mg) of L-PA **1**, 15 g cdw/L of *E. coli* (RFP-DEA-CGS), 20 g cdw/L of *E. coli* (EB-DGA), 20 mM glucose, 0.1 mM PLP, 400 mM L-Ala and 150 mM NH_3/NH_4Cl. The reactions were performed at 25°C and 250 rpm for 12 h. After the reactions were finished, the reaction mixtures were basified by adding NaOH (10 N) and extracted with ethyl acetate (EtOAc) for three times (3 × 50 mL). The organic phase was dried over anhydrous Na_2SO_4. The solvent was removed by evaporation and the residue was purified using a silica gel column with EtOAc/methanol (10:1) as eluent.

(*S*)-**7** was obtained as a white solid in 71.0 % yield (194.8 mg) and > 99% *ee*. ^{1}H NMR (400 MHz, 298K, $CDCl_3$) δ_H 7.34 – 7.26 (5H, m, Ph), 4.02 (1H, dd, $^3J_{HH}$ = 4.0 Hz, 8.5Hz, CH), 3.73–3.70 (1H, dd, $^2J_{HH}$ = 11.0Hz, $^3J_{HH}$ = 4.0 Hz, CH_2), 3.56–3.52 (1H, dd, $^2J_{HH}$ = 11.0Hz, $^3J_{HH}$ = 8.5 Hz, CH_2), 2.45 (br, 3H).

(*R*)-**7** was obtained as a yellow oil in 80.5% yield (220.9 mg) and > 99% *ee*. ^{1}H NMR (400 MHz, 298K, $CDCl_3$) δ_H 7.37 – 7.26 (5H, m, Ph), 4.07–4.03 (1H, dd, $^3J_{HH}$ = 4.0 Hz, 8.5Hz, CH), 3.76–3.72 (^{1}H, dd, $^2J_{HH}$ = 11.0Hz, $^3J_{HH}$ = 4.0 Hz, CH_2), 3.58–3.54 (1H, dd, $^2J_{HH}$ = 11.0Hz, $^3J_{HH}$ = 8.5 Hz, CH_2), 2.40 (br, 3H).

Assay methods

For GC analysis of styrene **3**, (*S*)-1-phenyl-1, 2-ethanediol **5** and 2-HAP **6**, the reaction samples (300 µL) were saturated with sodium chloride, mixed with 300 µL of EtOAc containing 20 mM of *n*-dodecane (internal standard), after centrifugation (12,000 rpm) at 4°C for 5 min, the organic phase was separated and dried over anhydrous Na_2SO_4. The concentration of styrene, (*S*)-1-phenyl-1, 2-ethanediol and 2-HAP were determined by GC analysis. For GC analysis of phenylglycinol **7**, the reaction samples (300 µL) were saturated with sodium chloride, and adjusted to pH = 12 with NaOH solution (10 N), and then extracted with EtOAc (300 µL) containing 20 mM of *n*-dodecane (internal standard). The organic phase was dried

over anhydrous Na_2SO_4, the concentration of the phenylglycinol **7** was determined by GC analysis. GC analysis was conducted using Shimadzu GC-14C gas chromatography system with a flame ionization detector. The column was an Agilent HP-5 (30 m × 0.32 mm × 0.25 mm). Parameter: injector temperature, 250^{o}C; detector temperature, 275°C; column temperature: 120°C. The enantiomeric excesss of (*S*)-phenylglycinol or (*R*)-phenylglycinol were determined by chiral GC as described previously (Zhang et al. 2020).

Results And Discussion

Design and in vitro **construction of the artificial biocatalytic cascade for conversion of L-PA 1 to chiral phenylglycinol 7**

To convert bio-based L-PA **1** to chiral phenylglycinol **7**, a sequential cascade biocatalysis was designed by retrosynthetic strategy (Scheme 1). First, L-PA **1** was deaminized to *trans*-cinnamic acid **2** by a phenylalanine ammonia lyase (PAL), followed by oxidative decarboxylation of *trans*-cinnamic acid **2** to styrene **3** by a phenylacrylic acid decarboxylase (PAD). Styrene **3** was subsequently oxidized to styrene oxide **4** by styrene monooxygenase (SMO), styrene oxide **4** was hydrolyzed to 1-phenyl-1,2-ethanediol **5** by an epoxide hydrolase (EH), 1-phenyl-1,2-ethanediol **5** was then oxidized to 2-HAP **6** by an alcohol dehydrogenase (ADH) and finally asymmetric reduction amination of 2-HAP **6** to chiral phenylglycinol **7** by an ω-transaminase (ωTA).

To reconstruct this cascade biocatalysis *in vitro*, PAL from *Arabidopsis thaliana* (Cochrane et al. 2004) which plays an important role in the process of ammonia removal was selected for conversion of L-PA **1** to *trans*-cinnamic acid **2**. In the second decarboxylation step, Fdc1 and Pad1 from *Aspergillus Niger* were selected for conversion of *trans*-cinnamic acid **2** to styrene **3**, the two enzymes can work together to decarboxylation of **2** more efficiently than either of them alone (Payne et al. 2015). In the third step, NADH dependent styrene monooxygenase (SMO) from *Pseudomonas* sp. VLB120 was employed for conversion of styrene **3** to (*S*)-styrene epoxide **4** (Xu et al. 2009). In the fourth step, epoxide hydrolase (SpEH) from *Sphingomonas* sp.HXN-200 was utilized to selective hydrolysis of **4** to (*S*)-diol **5** (Wu et al. 2013). In the fifth step, an NAD^+ dependent alcohol dehydrogenase (GoSCR) from *Glucoconobacter oxydans* 621H (Cui et al. 2017) was selected for oxidation of (*S*)-diol **5** to 2-HAP **6**. In the final amination step, an (*R*)-selective ω-transaminase (MVTA) from *Mycobacterium vanbaalenii* (Zhang et al. 2019) and an (*S*)-selective ω-transaminase (BMTA) from *Bacillus megaterium* SC6394 (Zhang et al. 2020) were employed to convert 2-HAP **6** to (*S*)-**7** and (*R*)-**7**, respectively. The NAD^+ and NADH recycling system was formed in the third and fifth step of the catalytic process. All the enzymes used in this study were lyophilized cell-free extracts, the activities of lyophilized enzymes were tested toward the corresponding substrates (Additional file 1: Table S3, PAL: 0.21 U/mg; Fdc1/Pad1: 0.95 U/mg; SMO: 0.28 U/mg; SpEH: 0.48 U/mg; GoSCR: 0.12 U/mg; MVTA: 3.10 U/mg; BMTA: 0.97 U/mg). Then, L-PA (10–20 mM) and NADH (0.5 mM) were added into the reaction system including the six different enzymes of PAL/Fdc1/Pad1/SMO/SpEH/GoSCR. Without optimizing the reaction conditions, 2-HAP **6** could be obtained in 99% conversion from 10–20 mM L-PA (Table 1, entry 1–2). In addition, the (*R*)-**7** and (*S*)-**7** could be obtained in > 99% *ee* and 66.8–

87.2% conversion from 10–20 mM L-PA with the mixture of seven different enzymes (PAL/Fdc1/Pad1/SMO/SpEH/GoSCR/MVTA or BMTA) (Table 1 entry 3–6). These results showed that the designed cascade biocatalysis was successfully constructed *in vitro* for conversion of L-PA **1** to chiral **7**. However, the *in vitro* cascade reactions need preparation of multiple enzymes, the cell-free enzymes are easily suffered from a rapid deactivation, and the redox reaction requires expensive cofactor (NAD^+/NADH), which will increase the cost of the reaction. Then we decided to construct recombinant *E. coli* whole cells which co-expression of necessary enzymes for conversion of L-PA **1** to chiral phenylglycinol **7**.

Table 1
Cascade biocatalysis for conversion of L-PA **1** to 2-HAP **6** and chiral phenylglycinol **7** with the mixture of lyophilized cell free extract.[a]

Entry	Sub.(mM)	Time (h)	Yield of 5 (%)[d]	Yield of 6 (%)[d]	Yield of 7 (%)[d]	*ee* of 7 (%)[e]
1	10[b]	7	< 1	99	-	-
2	20[b]	12	< 1	99	-	-
3	10[c]	12	16.1	< 1	83.0	> 99 (R)
4	20[c]	24	32.5	< 1	66.8	> 99 (R)
5	10[c]	12	2.6	10.2	87.2	> 99 (S)
6	20[c]	24	4.3	25.3	70.4	> 99 (S)

[a]The reactions were conducted in 5 mL sodium phosphate buffer (100 mM, pH 7.5). [b] The reactions containing 10–20 mM L-PA, 0.5 mM NADH, 15 mg/mL PAL, 15 mg/mL Fdc1, 15 mg/mL Pad1, 20 mg/mL SMO, 10 mg/mL SpEH, 20 mg/mL GoSCR, at 30°C and 200 rpm for 6 h. [c] The reactions containing 10–20 mM L-PA, 0.5 mM NADH, 15 mg/mL PAL, 15 mg/mL Fdc1, 15 mg/mL Pad1, 20 mg/mL SMO, 10 mg/mL SpEH, 20 mg/mL GoSCR, 15 mg/mL MVTA or 15 mg/mL BMTA, 0.1 mM PLP, (*R*)-MBA (15–25 mM) or L-alanine (200 mM), at 30°C and 200 rpm for 6 h. [d] Yield was determined by GC. [e] *ee* was determined by chiral GC.

Construction of recombinant E. coli cell modules for conversion of L-PA to 2-HAP

As we know, co-expression of multi-enzymes in one microbial cell will usually result in serious protein expression burden and redox constraints. While these negative factors can be reduced by distributing the biocatalytic pathway among different cell modules (Wang et al. 2020). Then, we decided to design and construction of synthetic microbial consortia to convert L-PA **1** to chiral phenylglycinol **7**. The microbial consortium for conversion of L-PA **1** to chiral **7** including two different recombinant *E. coli* cell modules (Scheme 1). One *E. coli* cell module co-expression of the PAL/PAD (Fdc1 and Pad1)/SMO/EH/GoSCR for conversion of L-PA **1** to 2-HAP **6**. The second recombinant *E. coli* cell module (module 2 or module 3) expressing an ω-TA for conversion of 2-HAP **6** to chiral phenylglycinol **7**. The recombinant *E. coli* cell module **2** expressing an (*R*)-selective ω-transaminase (MVTA) for conversion of 2-HAP **6** to (*S*)-**7**. The

recombinant *E. coli* cell module **3** co-expression of (*S*)-selective ω-transaminase (BMTA), alanine dehydrogenase (AlaDH) and glucose dehydrogenase (GDH) for conversion 2-HAP **6** to (*R*)-**7**.

Then, the recombinant *E. coli* cells module **1** co-expression of six enzymes (PAL/Fdc1/Pad1/SMO/SpEH/GoSCR) was constructed for conversion of L-PA **1** to 2-HAP **6**. Three expression plasmids (pETDuet-1, pRSFDuet-1, pCDFDuet-1) were used to co-expression of two different enzymes with various combinations (Additional file 1: Figure S1-S3). At last, three recombinant *E. coli* cells (*E. coli* (RFP-DEA-CGS), *E. coli* (DFP-CAS-REG), *E. coli* (CFP-DES-RGA)) with three different plasmids combinations co-expressing of six enzymes were successfully constructed (Fig. 1A), SDS-PAGE analysis of the crude lysate of the constructed recombinant *E. coli* cells showed that all six enzymes were successfully expressed in *E. coli* cells (Fig. 1B). The activities of the constructed recombinant *E. coli* cells for conversion of L-PA **1** to 2-HAP **6** were detected with 10 mM L-PA. The results showed that the recombinant *E. coli* (RFP-DEA-CGS) cells had the highest activity (5.6 U/g cdw) toward L-PA **1**. By using the recombinant *E. coli* (RFP-DEA-CGS) cells, the conversion of 2-HAP **6** could reach up to 93% within 7 h (Fig. 1C). Then, recombinant *E. coli* (RFP-DEA-CGS) was selected as the best candidate to convert L-PA **1** to 2-HAP **6**. The cell growth and specific activity of recombinant *E. coli* (RFP-DEA-CGS) were further analyzed, as shown in Fig. 1D, after 14 h induction, the highest activity of *E. coli* (RFP-DEA-CGS) could reach 5.8 U/g cdw with the OD_{600} of 3.0.

Convert L-PA 1 to 2-HAP 6 by E. coli (RFP-DEA-CGS)

After the recombinant *E. coli* (RFP-DEA-CGS) was selected for conversion L-PA to 2-HAP, the reaction conditions were optimized with 20 mM L-PA. The highest conversion of 2-HAP could reach 92% at pH 7.5 and 25^{o}C (Fig. 2A-B). Addition of 10 mM glucose could increase the conversion of 2-HAP **6** to 95% (Fig. 2C). For 10 mM L-PA **1**, 15 g cdw/L *E. coli* (RFP-DEA-CGS) was enough to convert L-PA **1** to 2-HAP **6** with 99% conversion. While 25 g cdw/L *E. coli* (RFP-DEA-CGS) was needed for conversion of 20 mM L-PA **1** to 2-HAP **6**. For 30 mM L-PA, 91.6% conversion of 2-HAP **6** was obtained by using 25 g cdw/L *E. coli* (RFP-DEA-CGS). For 50 mM L-PA, the conversion of 2-HAP **6** was decreased to 46.2%, even 25 g cdw/L of *E. coli* (RFP-DEA-CGS) was used (Fig. 2D, Additional file 1: Figure S4). 2-HAP **6** is a very important structural moiety in many synthetic intermediates in organic and medicinal chemistry. For example, 2-HAP can be used as a building block in the synthesis of oxazolone carboxamides, which is a novel class of acid ceramidase inhibitors, may act as useful pharmacological tools in relevant sphingolipid-mediated disorder (Caputo et al. 2020). In addition, 2-HAP itself as a potent inhibitor of urease (Tanaka et al. 2004).

Construction of recombinant E. coli cell modules for conversion of 2-HAP to chiral phenylglycinol

To bioconversion of 2-HAP **6** to (*S*)-**7**, an (*R*)-ωTA (MVTA) catalyzes the asymmetric amination of the 2-HAP **6** to (*S*)-**7** was selected, where by R-MBA serves as an optimum amine donor that leads to acetophenone (AP) as the by-product (Zhang et al. 2019a). The recombinant *E. coli* (MVTA) was then constructed for conversion of 2-HAP **6** to (*S*)-phenylglycinol **7**, the activity of recombinant *E. coli* (MVTA) cells was tested toward 2-HAP **6**, and 22.2 U/g cdw was obtained. To bioconversion of 2-HAP **6** to (*R*)-**7**,

an (*S*)-ωTA (BMTA) catalyzes the amination of the 2-HAP **6** to (*R*)-**7** was selected, whereby L-Ala serves as an optimum amine donor that leads to pyruvate. Pyruvate can then be recycled to alanine by employing an alanine dehydrogenase (AlaDH), which consumes ammonia and NADH, the NADH can be recycled using a glucose dehydrogenase (GDH). Then, recombinant *E. coli* cells co-expresssion of BMTA, AlaDH and GDH was constructed (Fig. 3A). SDS-PAGE showed that all the enzymes were successfully expressed (Fig. 3B). The activities of recombinant *E. coli* cells were tested with 10 mM 2-HAP **6**, the recombinant *E. coli* (EB-DGA) cells showed the highest activity (8.3 U/g cdw) toward 2-HAP **6**, and 95% conversion of (*R*)-**7** could be obtained after 12 h reaction (Fig. 3C).

Convert L-PA 1 to (S **)-7 by the designed** E. coli **(RFP-DEA-CGS) and** E. coli **(MVTA) consortium**

After the biocatalytic modules were constructed, the lyophilized *E. coli* (RFP-DEA-CGS) and *E. coli* (MVTA) cells were combined to convert L-PA **1** to (*S*)-**7**. The reaction conditions were first optimized with 20 mM of L-PA **1** substrate. As shown in Fig. 4A-E, combining *E. coli* (RFP-DEA-CGS) and *E. coli* (MVTA) at the ratio of 1:1 (15 g cdw/L of *E. coli* (RFP-DEA-CGS) and 15 g cdw/L of *E. coli* (MVTA)), the highest conversion of (*S*)-**7** (78%) was obtained at pH 7.5 and 25°C, with 10 mM glucose and 30 mM R-MBA were added. The adjustment of two recombinant *E. coli* cells at the ratio of 2:1.5 (20 g cdw/L of *E. coli* (RFP-DEA-CGS) and 15 g cdw/L of *E. coli* (MVTA)) resulted in the highest conversion of (*S*)-**7** (80%) in > 99% *ee*. Under the above optimized reaction conditions, different concentration of L-PA **1** (10–50 mM) were tested in a period of 7 h (Fig. 4F), 98% conversion of (*S*)-7 was obtained with 10 mM L-PA **1**. For 30 mM L-PA **1**, (*S*)-**7** was obtained in only 34.4% conversion. Further increase the substrate concentration to 50 mM, the conversion of (*S*)-**7** was sharply decreased to 12.9%, the remaining intermediate product was mainly diol **5** (85%), and almost no 2-HAP **6** was detected in the reaction mixture. We speculated that the reactivity of GoSCR towards diol intermediate in this cascade biocatalysis system was severely inhibited by R-MBA. Then, the effect of different concentration of R-MBA (0–60 mM) on the conversion of 2-HAP **6** by *E. coli* (RFP-DEA-CGS) was examined with 20 mM L-PA **1**. The results showed that the conversion of 2-HAP **6** was significantly decreased with the increasing concentration of R-MBA (Additional file 1: Figure S5).

The time course for the bioconversion of 10–30 mM L-PA **1** to (*S*)-**7** was shown in Fig. 5. (*S*)**-7** could be obtained in 99% and 84% conversion and > 99% *ee* from 10 mM and 20 mM L-PA at 12 h (Additional file 1: Figures S6 and S8), respectively. For 30 mM L-PA, the highest conversion of (*S*)**-7** was only 35% (Fig. 5A). Analysis of intermediate product produced from L-PA (20 mM) showed that the (*S*)-**7** (35%), diol **5** (35%), styrene **3** (8%) and 2-HAP **6** (5%) were the main products remained in the reaction system at 1 h, which mean that 83% of L-PA **1** was converted to styrene **3** due to the high activity of PAL and Fdc1 and Pad1. After 1 h, the concentration of diol **5** began to decrease, while the concentration of (*S*)-**7** was increased linearly. At 7 h, trace amount of diol **5** (< 1%) and 2-HAP **6** (< 1%) were detected in the reaction mixture, the conversion of (*S*)-**7** reached 75%. At 12 h, the conversion of (*S*)-**7** was continually increased to 84% (Fig. 5B).

Convert L-PA 1 to (R **)-7 by the designed** E. coli **(RFP-DEA-CGS) and** E. coli **(EB-DGA) consortium**

To convert L-PA **1** to (*R*)-**7**, the lyophilized *E. coli* (RFP-DEA-CGS) and *E. coli* (EB-DGA) cells were combined to form an *E. coli* microbial consortium. The reaction conditions were optimized. As shown in Fig. 6A-F, combining *E. coli* (RFP-DEA-CGS) and *E. coli* (MVTA) at the ratio of 1.5:2 (15 g cdw/L of *E. coli* (RFP-DEA-CGS) and 20 g cdw/L of *E. coli* (EB-DGA)), the highest conversion of (*R*)-**7** (85%) was obtained at pH 7.5 and 25^{o}C, with 20 mM glucose and 400 mM L-Ala added. In addition, providing the reaction mixture with 150 mM NH_3/NH_4Cl (regeneration of L-Ala by AlaDH) resulted in 95% conversion of (*R*)-**7**. The time course for the conversion of 10–30 mM L-PA **1** to (*R*)-**7** was shown in Fig. 7. (*R*)**-7** could be obtained in 99% and 95% conversion and > 99% *ee* from 10 mM and 20 mM L-PA at 12 h (Additional file 1: Figures S7-S8), respectively. For 30 mM L-PA, after 16 h reaction, (*R*)**-7** was obtained in 72.8% conversion and > 99% ee (Fig. 7A). Analysis of intermediate product produced from L-PA (20 mM) showed that the 2-HAP **6** (38.6%), (*R*)-**7** (26.2%), diol **5** (10.0%), styrene **3** (7%) were the main product remained in the reaction mixture at 1 h, which mean that > 84% of L-PA **1** was converted to styrene **3** due to the high activity of PAL and Fdc1 and Pad1, this is consistent with the above system for conversion of L-PA **1** to (*S*)**-7**. However, 2-HAP **6** (38.6%) remained in this reaction system is much more than diol **5** (10.0%), which mean that the most of diol **5** was converted to 2-HAP, and exhibited that the activity of GoSCR was not affected in this system. After 1 h reaction, the concentration of 2-HAP began to decrease, while the concentration of (*S*)-**7** was increased linearly. At 12 h, (*R*)-**7** was produced in 95% conversion and > 99% ee, trace amount of 2-HAP **6** (1.5%) was detected in the system, and the diol **5** and styrene **3** could not be detected at this time (Fig. 7B).

Preparation of (S)-7 and (R)-7 from L-PA

To examine the scalability of this cascade biocatalysis, preparative experiments were conducted on a 100 mL-scale via the constructed recombinant *E. coli* microbial consortium. After the reactions were finished (12 h), the reaction solution was extracted with ethyl acetate and flash chromatography, pure (*S*)-**7** and (*R*)-**7** were prepared with 71.0% and 80.5% isolated yields, > 99% *ee*, and 5.19 g/L.d and 4.42 g/L.d volumetric productivity, respectively (Table 2, Additional file 1: Figures S9-S10).

Table 2
Preparation of (*S*)-**7** and (*R*)-**7** from L-PA **1** with the combined resting cell of *E. coli* (RFP-DEA-CGS) and *E. coli* (MVTA) or *E. coli* (EB-DGA) [a]

Entry	L-PA 1 (mg)	Time (h)	7 (mg)	Yield of 7 (%)	*ee* of 7 (%)[b]	S.T.Y. (g/L.d)[c]
1	330.4	9	194.8	71.0	> 99(*S*)	5.19
2	330.4	12	220.9	80.5	> 99(*R*)	4.42

[a] The reactions were conducted in 100 mL sodium phosphate buffer (100 mM, pH 7.5). The reactions containing 2 mmol (330.4 mg) substrates, 20 g cdw/L *E. coli* (RFP-DEA-CGS) and 15 g cdw/L *E. coli* (MVTA) or 15 g cdw/L *E. coli* (RFP-DEA-CGS) and 20 g cdw/L *E. coli* (EB-DGA), 10–20 mM glucose, 0.1 mM PLP, 30 mM (*R*)-MBA or 400 mM L-Ala and 150 mM NH_3/NH_4Cl, at 25°C. [b] *ee* was determined by chiral GC. [c] S.T.Y.: space-time yield.

Conclusions

In conclusion, we successfully constructed a novel artificial biocatalytic cascade which was conducted by a recombinant *E. coli* microbial consortium to convert bio-based L-phenylalanine to chiral phenylglycinol. Seven kinds of enzymes (PAL/Pad1/Fdc1/SMO/SpEH/GoSCR/MVTA or BMTA) were first examined for the *in vitro* conversion of L-phenylalanine to synthesis of chiral phenylglycinol. (*R*)-phenylglycinol and (*S*)-phenylglycinol could be obtained in > 99% *ee* and 66.8–87.2% conversion from 10–20 mM L- phenylalanine. Recombinant *E. coli* microbial consortium including two recombinant *E. coli* cell modules was constructed for efficient conversion of L-phenylalanine to chiral phenylglycinol with good conversion (up to 99%) and excellent *ee* (> 99% *ee*). Moreover, the synthetic potential of this cascade biocatalysis was further confirmed by the constructed recombinant *E. coli* microbial consortium [*E. coli* (RFP-DEA-CGS)/*E. coli* (MVTA) or *E. coli* (RFP-DEA-CGS) /*E. coli* (EB-DGA)], (*S*)-phenylglycinol and (*R*)-phenylglycinol were obtained in good yields (71.0% and 80.5%) and > 99% *ee*. The salient features of this method are mild reaction conditions, good yields and excellent *ee*, no need for additional cofactor ($NADH/NAD^+$), providing a powerful entry to the sustainable synthesis of (*S*)-phenylglycinol or (*R*)-phenylglycinol from biobased L-phenylalanine.

Abbreviations

L-PA
L-phenylalanine; 2-HAP:2-hydroxyacetophenone; PAK4:p21-activated kinases; HDAC:histone deacetylase; PDK1:3-phosphoinositide-dependent protein kinase-1; AA:asymmetric aminohydroxylation; PAL:phenylalanine ammonia lyase; PAD:phenylacrylic acid decarboxylase, SMO:styrene monooxygenase, EH:epoxide hydrolase; ADH:alcohol dehydrogenase; MVTA:(*R*)-selective ω-transaminase from *Mycobacterium vanbaalenii*; BMTA:(*S*)-selective ω-transaminase from *Bacillus megaterium* SC6394; AlaDH:alanine dehydrogenase; GDH:glucose dehydrogenase; R-MBA:(*R*)-α-methylbenzylamine; PLP:pyridoxal-5'-phosphate; IPTG:isopropyl β-D-1-thiogalactopyranoside; LB:Luria-Bertani; TB:Terrific Broth; Fdc1:ferulic acid decarboxylase; Pad1:phenylacrylic acid decarboxylase; FID:flame ionization detector; GoSCR:polyol dehydrogenase from *Glucoconobacter oxydans* 621H; EtOAc:ethyl acetate; cdw:cell dry weight; L-Ala:L-alanine

Declarations

Acknowledgements

Not applicable.

Author contributions

JDZ conceived the idea and plan of this project. NQ performed most of the experiments. LLG performed part of the experiments in construction of dual-expression vectors. JL, FCZ and HHC performed part of

the experiments in the product analysis. JDZ supervised the whole research and revised the manuscript. All authors read and approved the final manuscript.

Funding

This study was supported by the National Natural Science Foundation of China (Grant No. 21772141), the Shanxi Province Science Foundation for Youths (grant No. 201701D221042), the Key Research and Development (R&D) Project of Shanxi Province (201803D31050).

Availability of data and materials

All data generated or analyzed during this study are included in this article.

Ethics approval and consent to participate

Not applicable.

Consent for publication

All authors approved the consent for publishing the manuscript to bioresources and bioprocessing.

Competing interests

The authors declare that they have no competing interests.

References

1. Becker J, Wittmann C (2012) Systems and synthetic metabolic engineering for amino acid production–the heartbeat of industrial strain development. Curr Opin Biotechnol 23: 718–726.
2. Bergmeier SC (2000) The synthesis of vicinal amino alcohols. Tetrahedron 56 (17): 2561–2576.
3. Bradford MM (1975) Rapid and sensitive method for quantitation of microgram quantities of protein utilizing principle of protein-dye binding. Anal Biochem 72: 248–254.
4. Caputo S, Di Martino S, Cilibrasi V, Tardia P, Mazzonna M, Russo D, Penna I, Summa M, Bertozzi SM, Realini N, Margaroli N, Migliore M, Ottonello G, Liu M, Lansbury P, Armirotti A, Bertorelli R, Ray SS, Skerlj R, Scarpelli R (2020) Design, synthesis, and biological evaluation of a series of oxazolone carboxamides as a novel class of acid ceramidase inhibitors. J Med Chem 63 (24): 15821–15851.
5. Chen FF, Cosgrove SC, Birmingham WR, Mangas-Sanchez J, Citoler J, Thompson MP, Zheng GW, Xu JH, Turner NJ (2019) Enantioselective synthesis of chiral vicinal amino alcohols using amine dehydrogenases. ACS Catal 9(12): 11813–11818.
6. Cochrane FC, Davin LB, Lewis NG (2004) The *Arabidopsis* phenylalanine ammonia lyase gene family: kinetic characterization of the four PAL isoforms. Phytochemistry 65: 1557–1564.

7. Cui ZM, Zhang JD, Fan XJ, Zheng GW, Chang HH, Wei WL (2017) Highly efficient bioreduction of 2-hydroxyacetophenone to (*S*)- and (*R*)-1-phenyl-1,2-ethanediol by two substrate tolerance carbonyl reductases with cofactor regeneration. J Biotechnol 243: 1–9.
8. Fotheringham I, Archer I, Carr R, Speight R, Turner NJ (2006) Preparative deracemization of unnatural amino acids. Biochem Soc Trans 34 (2): 287–290.
9. Gupta P, Mahajan N (2018) Biocatalytic approaches towards the stereoselective synthesis of vicinal amino alcohols. New J Chem 42 (15): 12296–12327.
10. Guo J, Zhu M, Wu TX, Hao CZ, Wang K, Yan ZZ, Huang WX, Wang J, Zhao DM, Cheng MS (2017) Discovery of indolin-2-one derivatives as potent PAK4 inhibitors: structure-activity relationship analysis, biological evaluation and molecular docking study. Bioorg Med Chem 25 (13): 3500–3511.
11. Jacobsen EN (2000) Asymmetric catalysis of epoxide ring-opening reactions. Acc Chem Res 33 (6): 421–431.
12. Kim S, Park JH, Koo SY, Kim JI, Kim MH, Kim JE, Jo K, Choi HG, Lee SB, Jung SH (2004) Novel diarylsulfonylurea derivatives as potent antimitotic agents. Bioorg Med Chem Lett 14 (24): 6075–6078.
13. Kobayashi S, Ishitani H, Ueno M (1998) Catalytic asymmetric synthesis of both syn-and anti-β-amino alcohols. J Am Chem Soc 120 (2): 431–432.
14. Lerchner A, Jarasch A, Skerra A (2016) Engineering of alanine dehydrogenase from *Bacillus subtilis* for novel cofactor specificity. Biotechnol Appl Biochem 63(5): 616–624.
15. Li G, Chang HT, Sharpless KB (1996) Catalytic asymmetric aminohydroxylation (AA) of olefins. Angew Chem Int Ed 35 (4): 451–453.
16. McKennon MJ, Meyers AI (1993) A convenient reduction of amino acids and their derivatives. J Org Chem 58 (13): 3568–3571.
17. Overman LE, Sugai S (1985) A convenient method for obtaining trans-2-aminocyclohexanol and trans-2-aminocyclopentanol in enantiomerically pure form. J Org Chem 50 (21): 4154–4155.
18. Panek JS, Masse CE (1998) An improved synthesis of (4*S*, 5*S*)-2-phenyl-4-(methoxycarbonyl)-5-isopropyloxazoline from (*S*)-phenylglycinol. J Org Chem 63 (7): 2382–2384.
19. Patel RN, Banerjee A, Howell JM, McNamee CG, Brozozowski D, Mirfakhrae D, Nanduri V, Thottathil JK, Szarka LJ (1993) Microbial synthesis of (2R,3S)-(−)-N-benzoyl-3-phenyl isoserine ethyl ester-a taxol side-chain synthon. Tetrahedron: Asymmetry 4 (9): 2069–2084.
20. Payne KA, White MD, Fisher K, Khara B, Bailey SS, Parker D, Rattray NJ, Trivedi DK, Goodacre R, Beveridge R, Barran P, Rigby SE, Scrutton NS, Hay S, Leys D (2015) New cofactor supports α, β-unsaturated acid decarboxylation via 1,3-dipolar cycloaddition. Nature 522: 497.
21. Pelckmans M, Renders T, Van de Vyver S, Sels BF (2017) Bio-based amines through sustainable heterogeneous catalysis. Green Chem 19 (22): 5303–5331.
22. Reetz MT (1991) New approaches to the use of amino acids as chiral building blocks in organic synthesis [new synthetic methods (85)]. Angew Chem Int Ed Engl 30 (12): 1531–1546.

23. Rouf A, Gupta P, Aga MA, Kumar B, Parshad R, Taneja SC (2011) Cyclic trans-β-amino alcohols: preparation and enzymatic kinetic resolution. Tetrahedron: Asymmetry 22 (24): 2134–2143.
24. Russell MGN, Matassa VG, Pengilley RR, van Niel MB, Sohal B, Watt AP, Hitzel L, Beer MS, Stanton JA, Broughton HB, Castro JL (1999) 3-[3-(Piperidin-1-yl)propyl]indoles as highly selective h5-HT1D receptor agonists. J Med Chem 42 (24): 4981–5001.
25. Schmidt F, Keller F, Vedrenne E, Aggarwal VK (2009) Stereocontrolled synthesis of β-amino alcohols from lithiated aziridines and boronic esters. Angew Chem Int Ed 48 (6): 1149–1152.
26. Sekar BS, Mao J, Lukito BR, Wang Z, Li Z (2020) Bioproduction of enantiopure (*R*)- and (*S*)-2-phenylglycinols from styrenes and renewable feedstocks. Adv Synth Catal 363 (7): 1892–1903.
27. Sharpless KB, Patrick DW, Truesdale LK, Biller SA (1975) New reaction. Stereospecific vicinal oxyamination of olefins by alkyl imido osmium compounds. J Am Chem Soc 97 (8): 2305–2307.
28. Studte C, Breit B (2008) Zinc-catalyzed enantiospecific sp3–sp3 cross-coupling of α-hydroxy ester triflates with grignard reagents. Angew Chem Int Ed 47 (29): 5451–5455.
29. Tan Q, Wang X, Xiong Y, Zhao Z, Li L, Tang P, Zhang M (2017) Chiral amino alcohol accelerated and stereocontrolled allylboration of iminoisatins: highly efficient construction of adjacent quaternary stereogenic centers. Angew Chem Int Ed 56 (17): 4829–4833.
30. Tan X, Zhang S, Song W, Liu J, Gao C, Chen X, Liu L, Wu J (2021) A multi-enzyme cascade for efficient production of D-p-hydroxyphenylglycine from L-tyrosine. Bioresour Bioprocess 8: 41.
31. Tanaka T, Kawase M, Tani S (2004) α-Hydroxy ketones as inhibitors of urease. Bioorg Med Chem 12 (2): 501–505.
32. Vandekerkhove A, Claes L, De Schouwer F, Van Goethem C, Vankelecom IFJ, Lagrain B, De Vos DE (2018) Rh-catalyzed hydrogenation of amino acids to biobased amino alcohols: tackling challenging substrates and application to protein hydrolysates. ACS Sustainable Chem Eng 6 (7): 9218–9228.
33. Wang F, Zhao J, Li Q, Yang J, Li R, Min J, Yu X, Zheng GW, Yu HL, Zhai C, Acevedo-Rocha CG, Ma L, Li A (2020) One-pot biocatalytic route from cycloalkanes to α, ω-dicarboxylic acids by designed *Escherichia coli* consortia. Nat Commun 11(1): 1–10.
34. Wang X, Su R, Chen K, Xu S, Feng J, Ouyang P (2019) Engineering a microbial consortium based whole-cell system for efficient production of glutarate from L-lysine. Front Microbiol 10: 341.
35. Wu HL, Zhang JD, Zhang CF, Fan XJ, Chang HH, Wei WL (2017) Characterization of four new distinct ω-transaminases from *Pseudomonas putida* NBRC 14164 for kinetic resolution of racemic amines and amino alcohols. Appl Biochem Biotechnol 181 (3) 972–985.
36. Wu S, Li A, Chin YS, Li Z (2013) Enantioselective hydrolysis of racemic and meso-epoxides with recombinant *Escherichia coli* expressing epoxide hydrolase from *Sphingomonas* sp. HXN-200: preparation of epoxides and vicinal diols in high *ee* and high concentration. ACS Catal 3 (4): 752–759.
37. Xu Y, Jia X, Panke S, Li Z (2009) Asymmetric dihydroxylation of aryl olefins by sequential enantioselective epoxidation and regioselective hydrolysis with tandem biocatalysts. Chem Commun 1481–1483.

38. You ZN, Zhou K, Han Y, Yang BY, Chen Q, Pan J, Qian XL, Li CX, Xu JH (2021) Design of a self-sufficient hydride-shuttling cascade for concurrent bioproduction of 7, 12-dioxolithocholate and L-*tert*-leucine. Green Chem 23(11): 4125–4133.
39. Zhang JD, Wu HL, Meng T, Zhang CF, Fan XJ, Chang HH, Wei WL (2017) A high-throughput microtiter plate assay for the discovery of active and enantioselective amino alcohol-specific transaminases. Anal Biochem 518: 94–101.
40. Zhang JD, Zhao JW, Gao LL, Chang HH, Wei WL, Xu JH (2019a) Enantioselective synthesis of enantiopure β-amino alcohols via kinetic resolution and asymmetric reductive amination by a robust transaminase from *Mycobacterium vanbaalenii*. J Biotechnol 290: 24–32.
41. Zhang JD, Yang XX, Jia Q, Zhao JW, Gao LL, Gao WC, Chang HH, Wei WL, Xu JH (2019b) Asymmetric ring opening of racemic epoxides for enantioselective synthesis of (S)-β-amino alcohols by a cofactor self-sufficient cascade biocatalysis system. Catal Sci Technol 9 (1): 70–74.
42. Zhang JD, Zhao JW, Gao LL, Zhao J, Chang HH, Wei WL (2019c) One-pot three-step consecutive transformation of L-α-amino acids to (*R*)- and (*S*)-vicinal 1,2-diols via combined chemical and biocatalytic process. ChemCatChem 11 (20): 5032–5037.
43. Zhang JD, Yang XX, Dong R, Gao LL, Li J, Li X, Huang SP, Zhang CF, Chang HH (2020) Cascade biocatalysis for regio- and stereoselective aminohydroxylation of styrenyl olefins to enantiopure arylglycinols. ACS Sustainable Chem Eng 8 (49): 18277–18285.
44. Zhou Y, Wu S, Li Z (2016) Cascade biocatalysis for sustainable asymmetric synthesis: from biobased L-phenylalanine to high-value chiral chemicals. Angew Chem Int Ed 128 (38): 11819–11822.

Figures

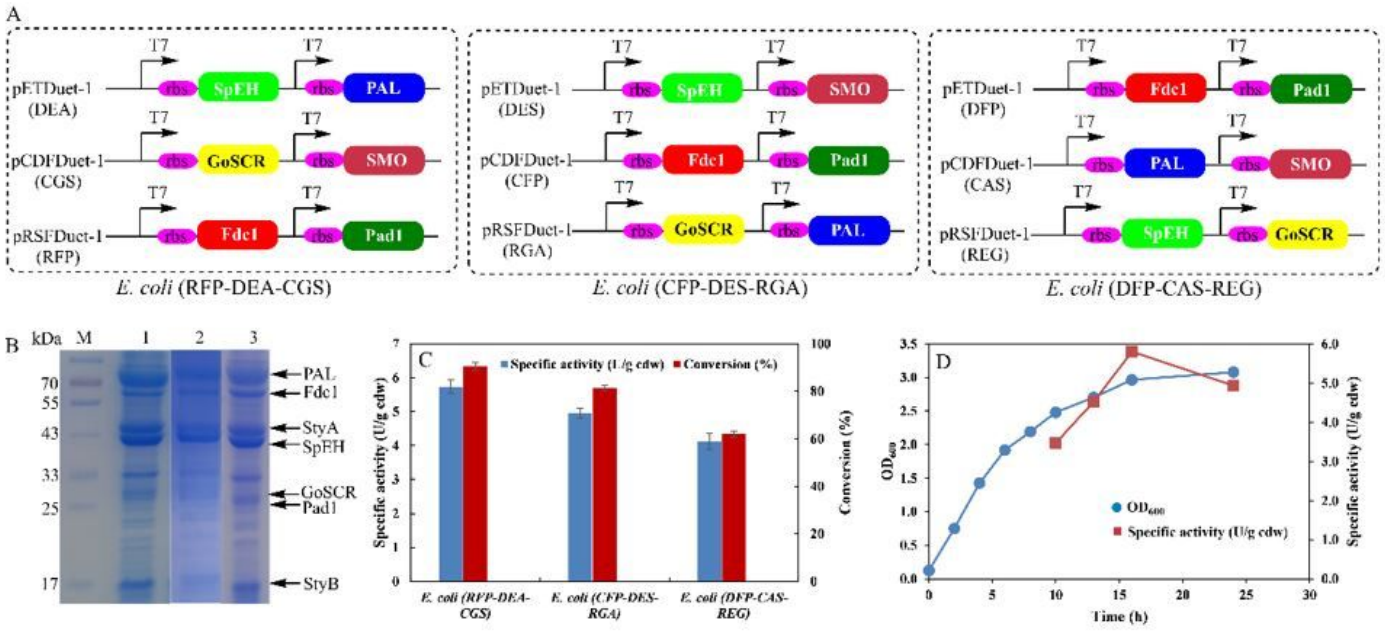

Figure 1

Construction of recombinant E. coli cells co-expression of six enzymes for conversion of L-PA 1 to 2-HAP 6. A: Construction of recombinant E. coli cells co-expression of six enzymes based on different plasmid configurations. B: SDS-PAGE analysis of recombinant E. coli cells. M: marker; lane 1: cell free extract of E. coli (RFP-DEA-CGS), lane 2: cell free extract of E. coli (CFP-DES-RGA); lane 3: cell free extract of E. coli (DFP-CAS-REG). C: Activities of three different recombinant E. coli cells for conversion of L-PA 1 to 2-HAP 6. D: Cell growth and specific activity of E. coli (RFP-DEA-CGS) for conversion of L-PA 1 to 2-HAP 6.

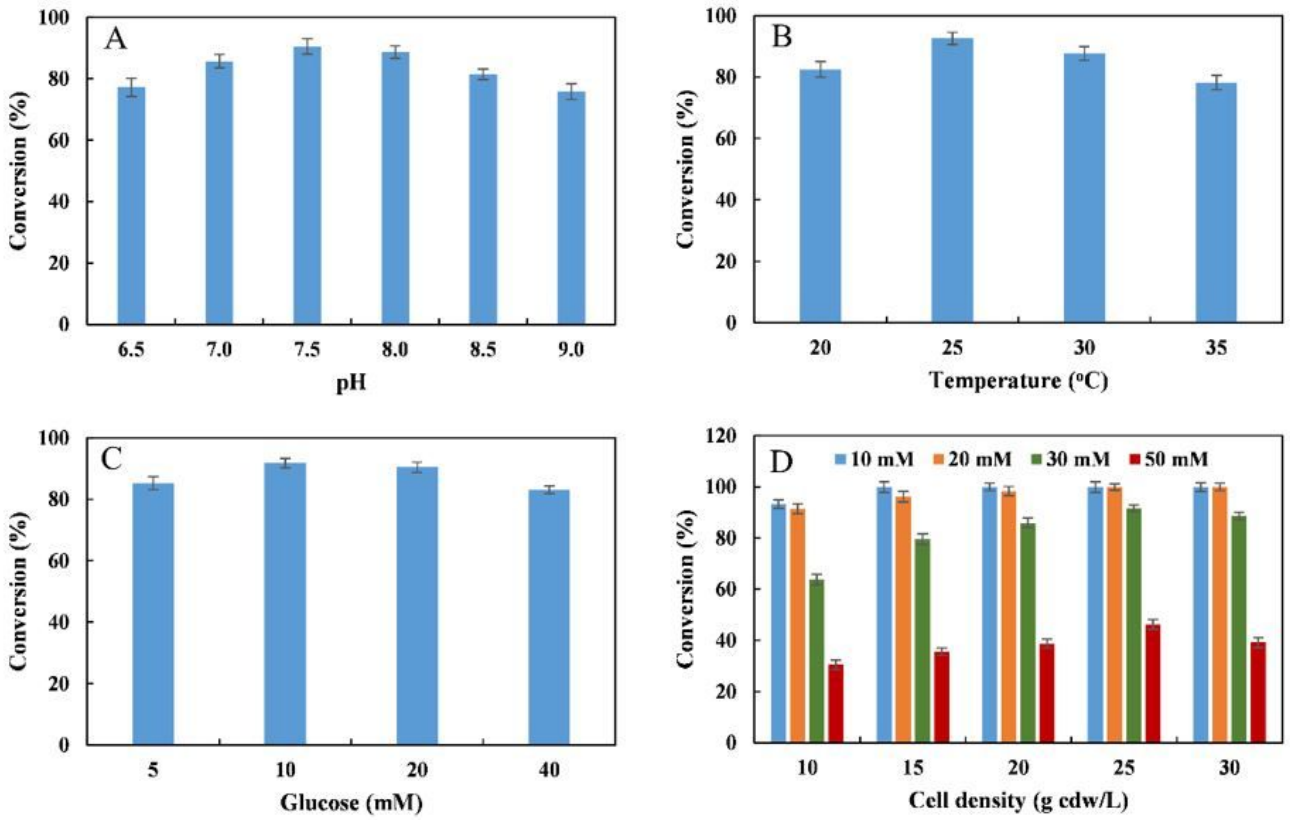

Figure 2

Reaction condition optimization for conversion of L-PA 1 to 2-HAP 6. A: Effect of different pH on the conversion of 2-HAP 6; B: Effect of different temperature on the conversion of 2-HAP 6; C: Effect of glucose concentration on the conversion of 2-HAP 6; D: Effect of different cell density of E. coli (RFP-DEA-CGS) on the conversion of different concentration of L-PA 6, blue: 10 mM of L-PA; yellow: 20 mM of L-PA; green: 30 mM of L-PA; red: 50 mM of L-PA.

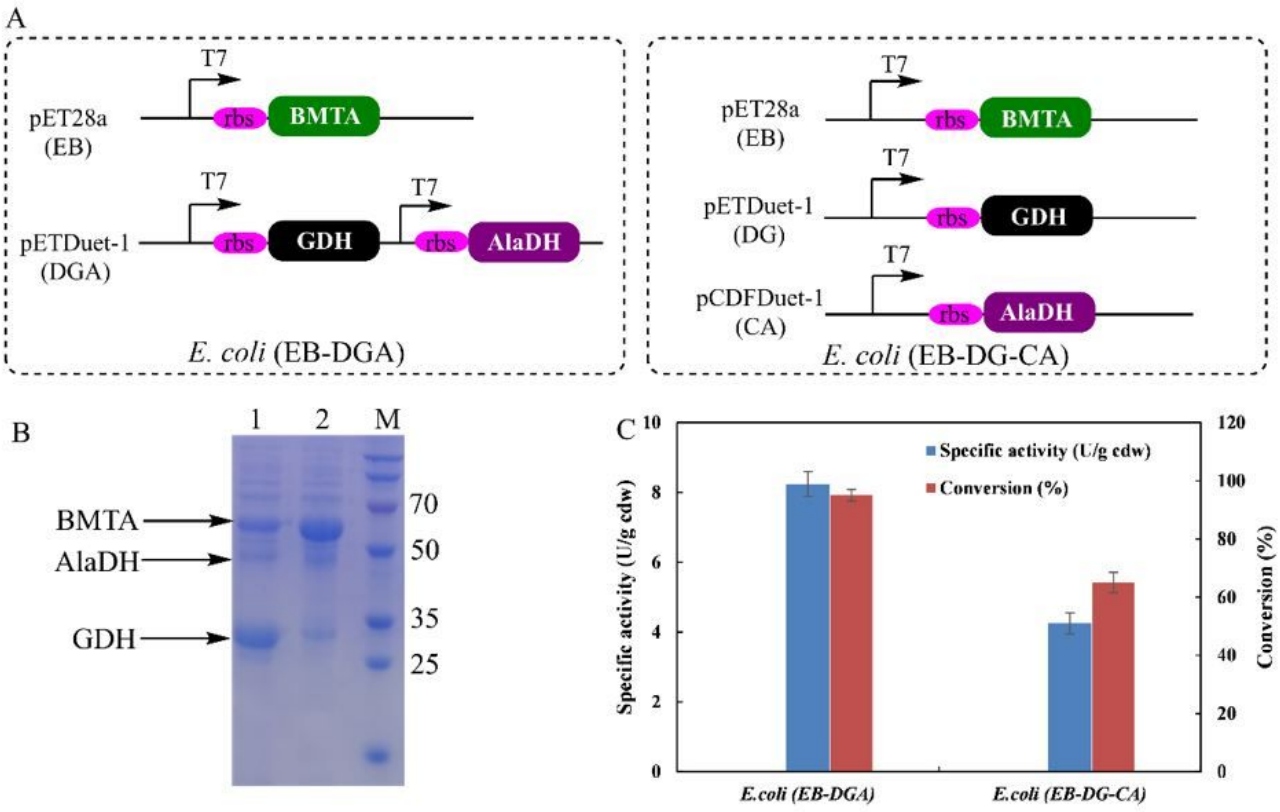

Figure 3

Construction of recombinant E. coli cells for conversion of 2-HAP 6 to (R)-phenylglycinol 7. A: Construction of recombinant E. coli cells co-expression of three enzymes (BMTA, AlaDH and GDH) based on different plasmid configurations. B: SDS-PAGE analysis of recombinant E. coli cells. M: marker; lane 1: cell free extract of E. coli (EB-DGA), lane 2: cell free extract of E. coli (EB-DG-CA). C: Activities of two different recombinant E. coli cells for conversion of 2-HAP 6 to (R)-phenylglycinol 7.

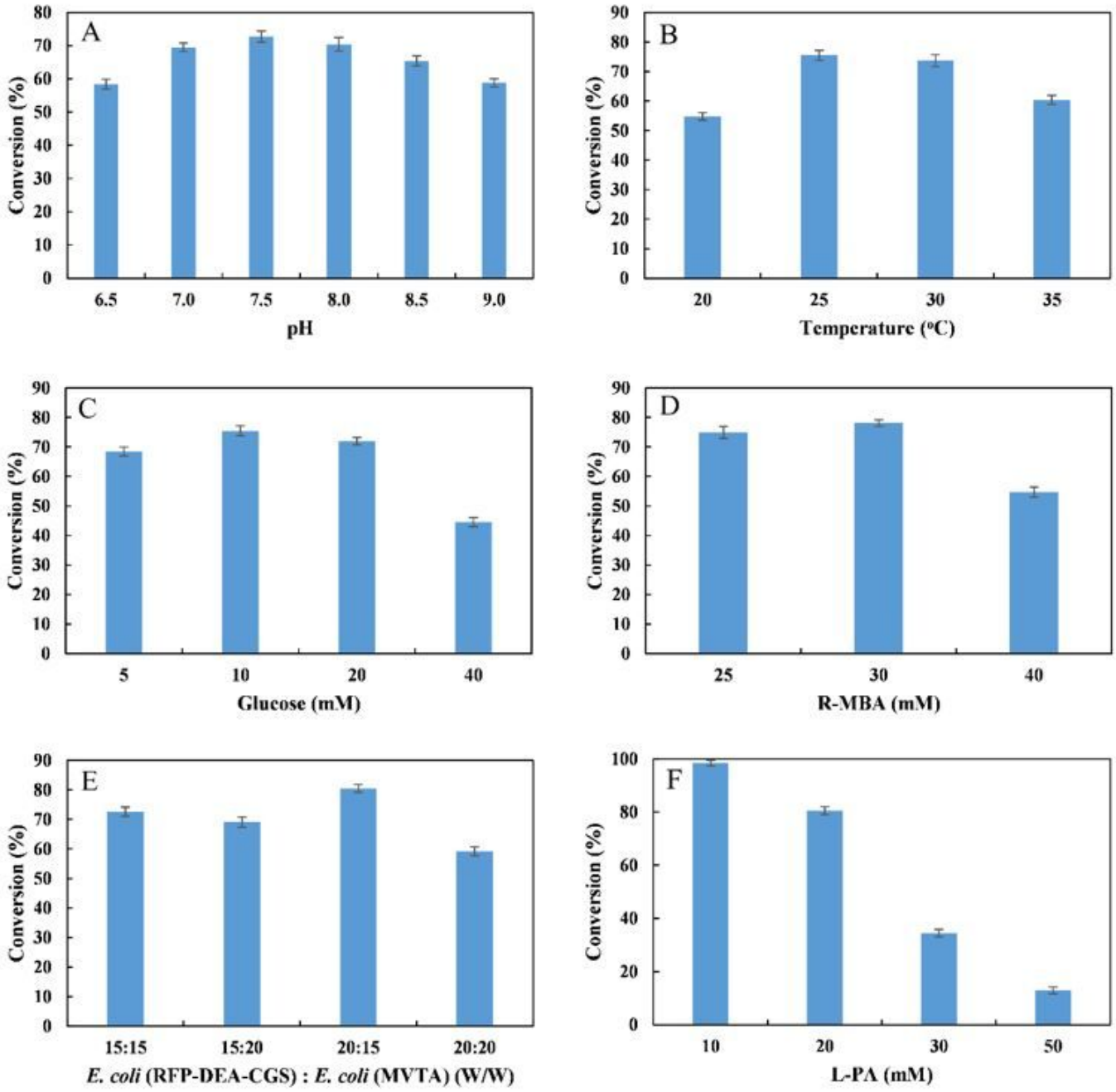

Figure 4

Reaction condition optimization for conversion of L-PA 1 to (S)-7 by the designed E. coli (RFP-DEA-CGS) and E. coli (MVTA) consortium. A: Effect of different pH on the conversion of (S)-7; B: Effect of different temperature on the conversion of (S)-7; C: Effect of glucose concentration on the conversion of (S)-7; D: Effect of R-MBA concentration on the conversion of (S)-7; E: Effect of different cell density of E. coli (RFP-DEA-CGS) and E. coli (MVTA) on the conversion of (S)-7; F: Effect of different L-PA 1 concentration on the conversion of (S)-7.

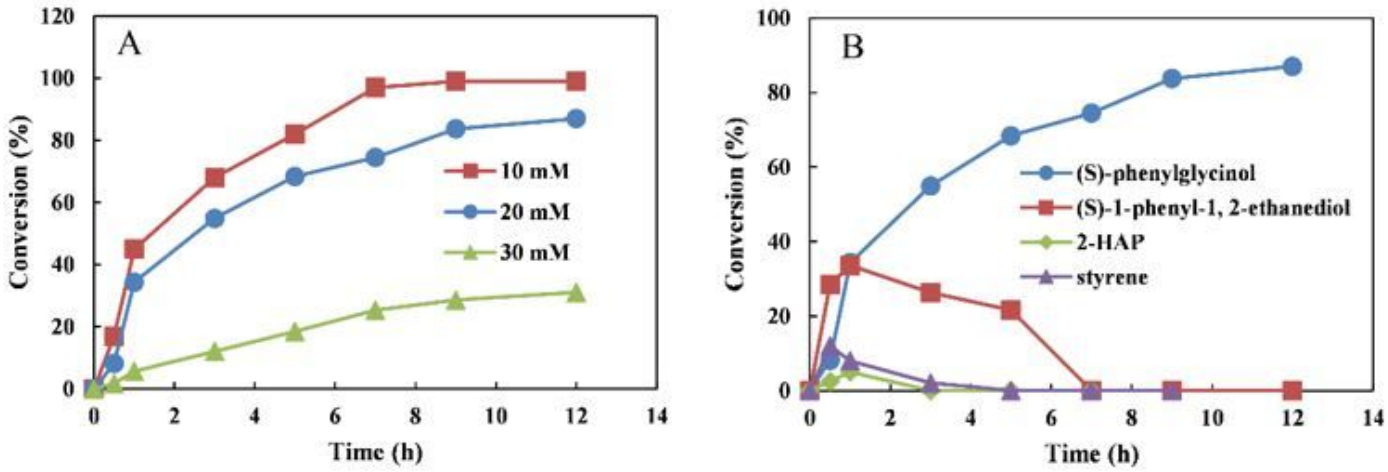

Figure 5

Time course of the cascade reaction for the synthesis of (S)-7 from L-PA 1. A: Time course of the cascade reaction for conversion of 10-30 mM L-PA 1 to (S)-7; B: Time course of the cascade reaction for intermediate produced from L-PA 1. Reaction conditions (5 mL): 100 mM phosphate buffer (pH 7.5), 10-30 mM L-PA, 10 mM glucose, 20 g cdw/L E. coli (RFP-DEA-CGS), 15 g cdw/L E. coli (MVTA), 30 mM (R)-MBA and 0.1 mM PLP, at 25 °C. All biotransformations were performed in duplicate and conversion was determined by GC, error limit: <2% of the state values.

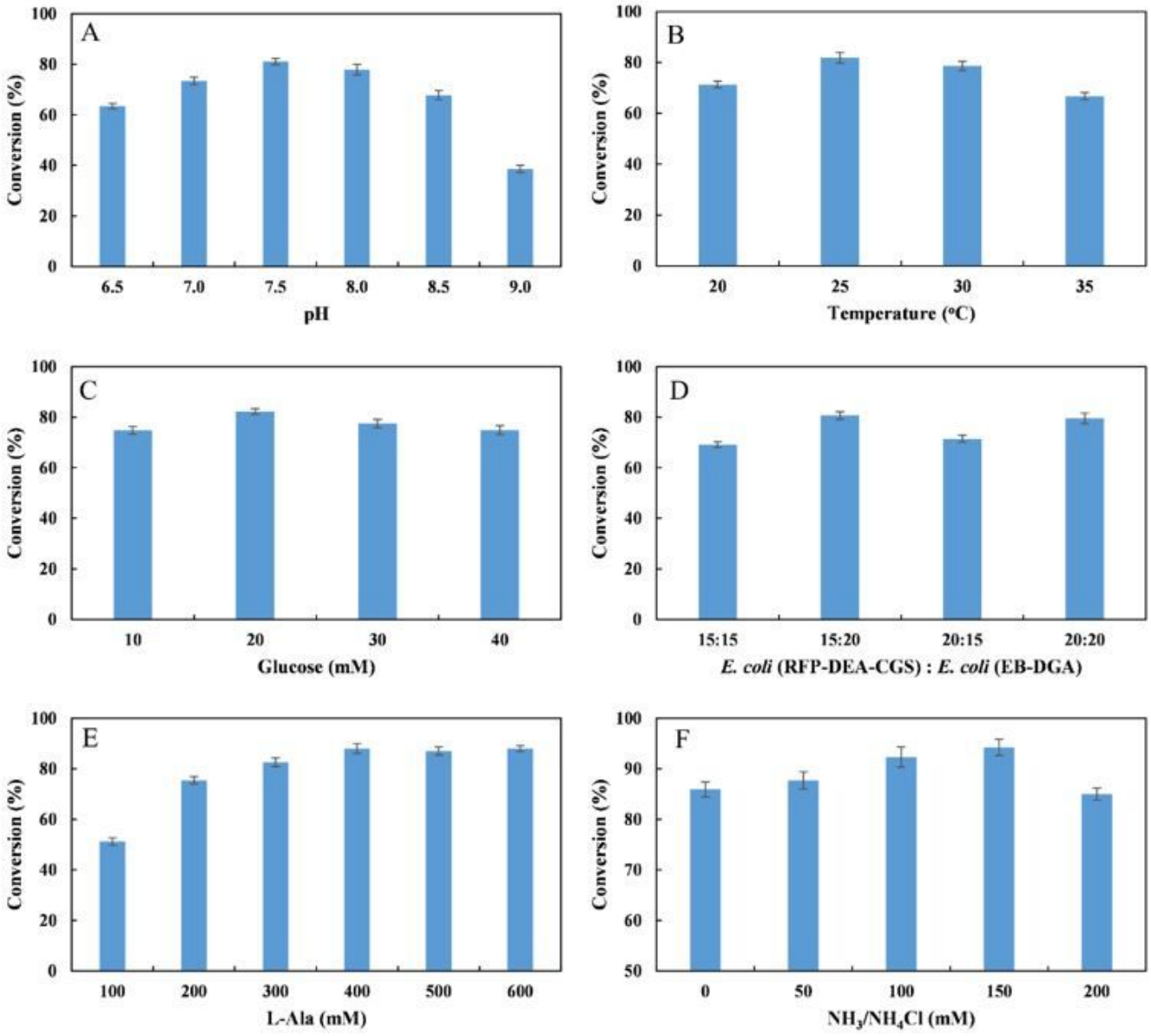

Figure 6

Reaction condition optimization for conversion of L-PA 1 to (R)-7 by the designed E. coli (RFP-DEA-CGS) and E. coli (EB-DGA) consortium. A: Effect of different pH on the conversion of (R)-7; B: Effect of different temperature on the conversion of (R)-7; C: Effect of glucose concentration on the conversion of (R)-7; D: Effect of different cell density of E. coli (RFP-DEA-CGS) and E. coli (MVTA) on the conversion of (R)-7; E: Effect of L-Ala concentration on the conversion of (R)-7; F: Effect of NH3/NH4Cl concentration on the conversion of (R)-7.

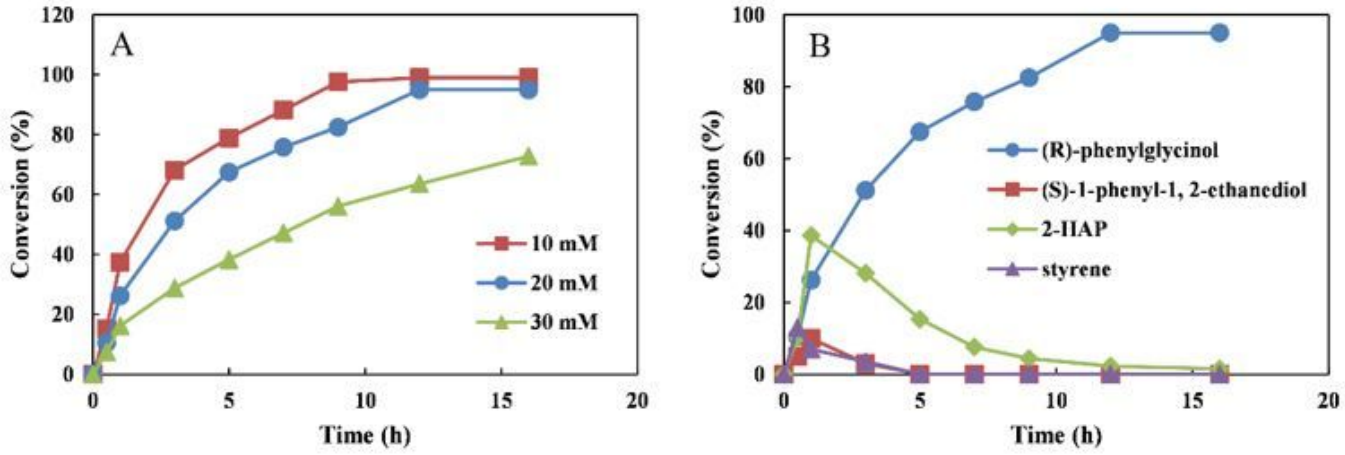

Figure 7

Time course of the cascade reaction for the synthesis of (R)-7 from L-PA 1. A: Time course of the cascade reaction for conversion of 10-30 mM L-PA to (R)-7; B: Time course of the cascade reaction for intermediate produced from L-PA 1. Reaction conditions (5 mL): 100 mM phosphate buffer (pH 7.5), 10-30 mM L-PA, 20 mM glucose, 15 g cdw/L E. coli (RFP-DEA-CGS), 20 g cdw/L E. coli (EB-DGA), 400 mM L-ala, 150 mM NH_3/NH_4Cl, 0.1 mM PLP, at 25 °C. All biotransformations were performed in duplicate and conversion was determined by GC, error limit: <2% of the state values.

Supplementary Files

This is a list of supplementary files associated with this preprint. Click to download.

- S1.jpg
- Graphcabstract.docx
- SupplementaryMaterial.docx